



HAL
open science

Laser written 3D 3T spectro-interferometer: study and optimisation of the laser-written nano-antenna

Myriam Bonduelle, Guillermo Martin, Irene Heras Perez, Alain Morand, Ciro d'Amico, Razvan Stoian, Guodong Zhang, Guanghua Cheng

► **To cite this version:**

Myriam Bonduelle, Guillermo Martin, Irene Heras Perez, Alain Morand, Ciro d'Amico, et al.. Laser written 3D 3T spectro-interferometer: study and optimisation of the laser-written nano-antenna. SPIE Astronomical Telescopes + Instrumentation,, Dec 2020, Online Only, France. pp.82, 10.1117/12.2562179 . hal-03101610

HAL Id: hal-03101610

<https://hal.univ-grenoble-alpes.fr/hal-03101610v1>

Submitted on 7 Jan 2021

HAL is a multi-disciplinary open access archive for the deposit and dissemination of scientific research documents, whether they are published or not. The documents may come from teaching and research institutions in France or abroad, or from public or private research centers.

L'archive ouverte pluridisciplinaire **HAL**, est destinée au dépôt et à la diffusion de documents scientifiques de niveau recherche, publiés ou non, émanant des établissements d'enseignement et de recherche français ou étrangers, des laboratoires publics ou privés.

PROCEEDINGS OF SPIE

[SPIDigitalLibrary.org/conference-proceedings-of-spie](https://spiedigitallibrary.org/conference-proceedings-of-spie)

Laser written 3D 3T spectro-interferometer: study and optimisation of the laser-written nano-antenna

Bonduelle, Myriam, Martin, Guillermo, Heras Perez, Irene, Morand, Alain, d'Amico, Ciro, et al.

Myriam Bonduelle, Guillermo Martin, Irene Heras Perez, Alain Morand, Ciro d'Amico, Razvan Stoian, Guodong Zhang, Guanghua Cheng, "Laser written 3D 3T spectro-interferometer: study and optimisation of the laser-written nano-antenna," Proc. SPIE 11446, Optical and Infrared Interferometry and Imaging VII, 114462T (13 December 2020); doi: 10.1117/12.2562179

SPIE.

Event: SPIE Astronomical Telescopes + Instrumentation, 2020, Online Only

Laser written 3D 3T spectro-interferometer: Study and optimisation of the laser-written nano-antenna

Myriam Bonduelle^a, Guillermo Martin^a, Irene Heras Perez^a, Alain Morand^b, Ciro d'Amico^c, Razvan Stoian^c, Guodong Zhang^{c,d}, and Guanghua Cheng^{c,d}

^aUniv. Grenoble Alpes, CNRS, IPAG, 38000 Grenoble, France

^bUniv. Grenoble Alpes, CNRS, Grenoble INP**, IMEP-LAHC, F-38000, Grenoble, France

^cLaboratoire Hubert Curien, UMR 5516 CNRS, Université de Lyon, Université Jean Monnet, 42000 St. Etienne, France

^dState Key Laboratory of Transient Optics and Photonics, Xi'an Institute of Optics and Precision Mechanics, CAS, 710119 Xi'an, Shaanxi, China

ABSTRACT

Stationary Wave Integrated Fourier Transform Spectrometers (SWIFTS) are based on the sampling of a stationary wave using nano-sampling centres on the surface of a channel waveguide. Single nanogroove sampling centres above the waveguide surface will radiate the sampled signal with wide angular distribution, which is not compatible with the buried detection area of infrared detectors, resulting in crosstalk between pixels. An implementation of multiple diffraction nano-grooves (antenna) for each sampling position is proposed as an alternative solution to improve directivity towards the detector pixel by narrowing the scattering angle of the extracted light. Its efficiency is demonstrated from both simulated and measured far field radiative patterns exhibiting a promising method to be used for future integrated IR-SWIFTS.

The implementation of the antennas will allow for a high resolution spectrometer in Infra-Red (here 1550nm) with no crosstalk problem (ref. [1]). These antennas, combined with the technology used (direct laser writing) will provide a robust, low-cost efficient tool that can be implemented as a 3D-3T spectro-interferometer (multi telescope beam-combiner), useful for astrophysics applications, such as phase closure studies.

1. GENERAL PRESENTATION

1.1 SWIFT'S Principle

The SWIFTS (Stationary Wave Integrated Fourier Transform Spectrometer) (ref. [2]) technology relies on the sampling of a stationary light wave by means of scattering nanogrooves. The wave enters a single-mode waveguide, is reflected on a mirror at the end of it, and by interference of the forward and backward optical beams, creates a stationary wave (i.e. a static interferogram). The interferogram is then sampled by the nanosampling centres (di-electric discontinuities), periodically placed in the evanescent field of the stationary wave. Using the discrete and periodical sampled values of the interferogram, through a Fourier Transform, the spectrum of the source can be reconstructed.

SWIFTS spectrometers are compact, and do not require any relay optics. It is also a very high resolution spectrometer : $R = \frac{2nL}{\lambda}$, with L the sampling length : for L = 1mm, lambda = 1,55 microns, n =1,44, R = 1858

The interferogram has a period of :

$$\frac{\lambda}{2n}, \text{ with } \lambda \text{ the wavelength, } n \text{ the refractive index} \quad (1)$$

In order to correctly sample the wave, the Shannon-Nyquist criteria has to be respected : the sampling period has to be inferior or equal to $\frac{\lambda}{4n}$ in order to avoid aliasing. This value is therefore the maximum distance that we can have between two sampling centres (two antennas).

Further author information: Send correspondence to myriam.bonduelle@univ-grenoble-alpes.fr

Optical and Infrared Interferometry and Imaging VII, edited by Peter G. Tuthill, Antoine Mérand, Stephanie Sallum, Proc. of SPIE Vol. 11446, 114462T · © 2020 SPIE
CCC code: 0277-786X/20/\$21 · doi: 10.1117/12.2562179

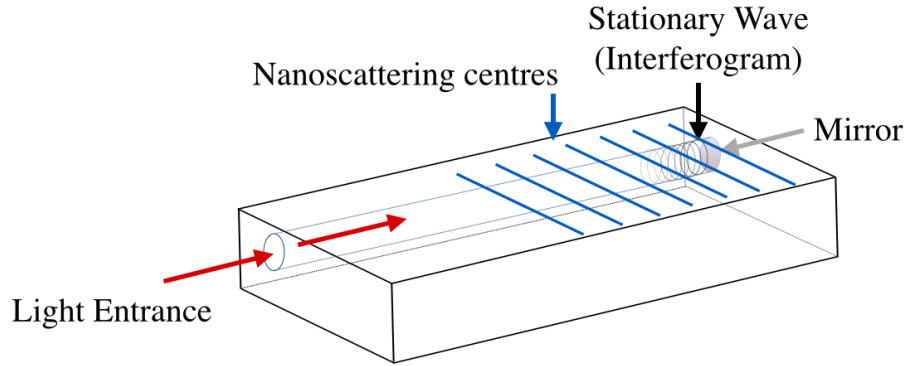


Figure 1. SWIFTS principle showing the waveguide, the mirror at the output, and the nanosampling centres

1.2 Adaptation in the Infra-Red

The chosen material for the sample is borosilicate glass, with a refractive index around 1,444 for the wavelength 1,55 μm . From this we can have the maximum period allowed between two sampling centres :

$$\frac{\lambda}{4n} \rightarrow \frac{1.55}{4 * 1.444} = 0.268 \mu m = 268 \text{ nm} \frac{\lambda}{2n}, \quad (2)$$

With the chosen technology (ultrafast laser writing), such a pitch cannot be obtained. Therefore the wave will necessarily be under-sampled. In order to solve that problem, an offset, spatial or temporal, will be introduced. A temporal offset can be obtained through the use of electrooptical materials, such as Lithium Niobate. A spatial offset can be obtained by sampling the wave using several waveguides rather than one and introducing a spatial shift:

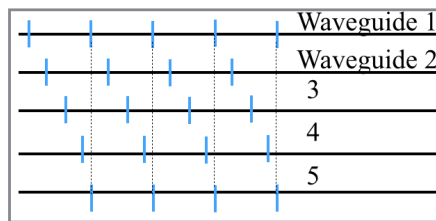


Figure 2. Spatial Offset

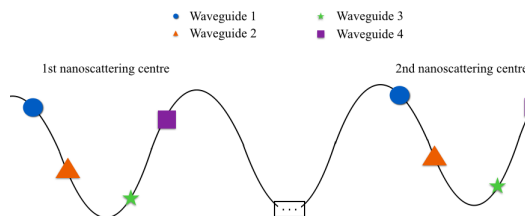


Figure 3. Sampling with a spatial offset

Each waveguide has its own set of sampling centres, that are shifted in comparison to the other waveguides. With the multiplexing of the four first waveguides, the sampling can be correctly done (i.e. four sampled values for one optical period).

As the aim is IR adaptation, the problematic of the detectors arise. The detection zone is deeply buried (a few hundreds of microns) in a semi-conductor layer, which is not the case in visible detectors. Because of this, there will be crosstalk : each nanosampling centre will radiate on several pixels of the detector, and will be mixed with

the signal from other centres.

In order to avoid this problem, instead of one groove per nanosampling centre, we will have several grooves per sampling centre. It will improve the directivity of each centre. In order to have each groove of the same sampling centre sample the same part of the wave, therefore creating a constructive interference, they have to have a pitch of an integer number of $\frac{\lambda}{n}$. (ref [3]).

1.3 Design and fabrication of the samples

In order to determine the ideal parameters for the SWIFTS spectrometer, samples were made with different combination of the following parameters : number of grooves per sampling centre, burial depth of the waveguide in respect to the grooves :

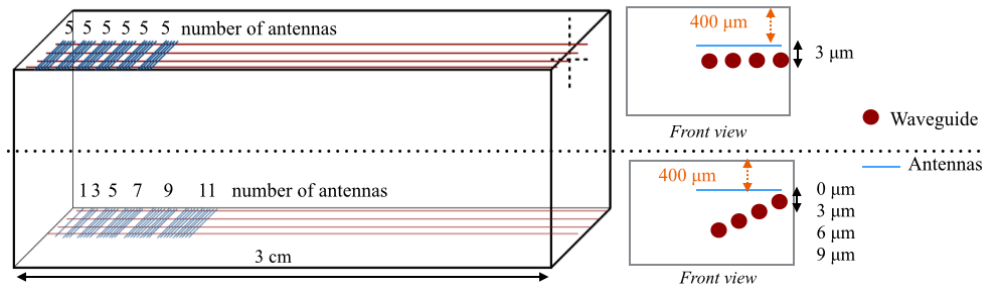


Figure 4. The two-sided sample

The first side has 5 grooves per antenna, always the same number, and each waveguide is around $3 \mu m$ under the grooves. The second face has different number of grooves per sampling centres (1, 3, 5, 7, 9, 11), and different distances waveguides / grooves : 0, 3, 6, 9 μm .

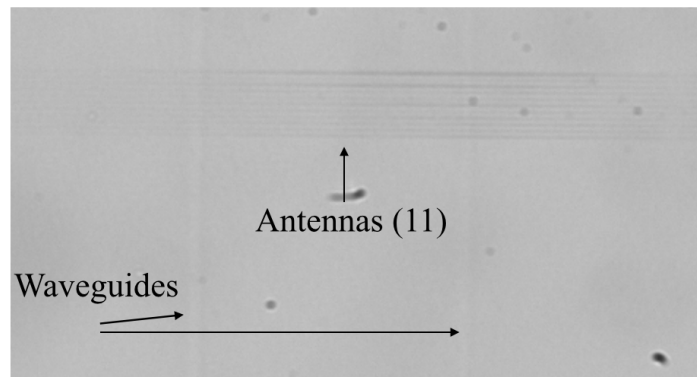


Figure 5. White light vue of the sample (2nd side) : group with 11 grooves

The samples were made at the Hubert Curien laboratory in Saint-Etienne, France. The waveguides are created by translating the sample during a laser irradiation. The grooves are created by generating non propagative and non-limited by diffraction Bessel beams. (ref [4]) This allows the grooves to be of nanometric scale, however the pitch between two consecutive grooves cannot be of $\frac{\lambda}{n}$, due to overlapping between Bessel holes. Therefore, the pitch had to be a multiple of $\frac{\lambda}{n}$, and the smallest value that was possible to obtain was $3 * \frac{\lambda}{n}$: 3 microns. There are many advantages to this technology : the guides and antennas can be buried, meaning that the sample will be less fragile and more easily handled. It is a rapid and simple technology, usable for many materials. The light propagated in the waveguides and the sampling centre (here containing 11 grooves) extract the light.

2. EXPERIMENTS

2.1 Far-field experiments

The first set of experiments are far-field experiments. The sample is observed through a microscope objective in order to have an overview of the results given by the different antennas (groove groups). This set-up aims to study all the different combination provided by the sample's design. The parameters are the number of grooves per sampling group, the distance between the grooves and the waveguides and the wavelength.

The best result is expected with the 11 grooves group : the wider the grating, the thinner the signal.

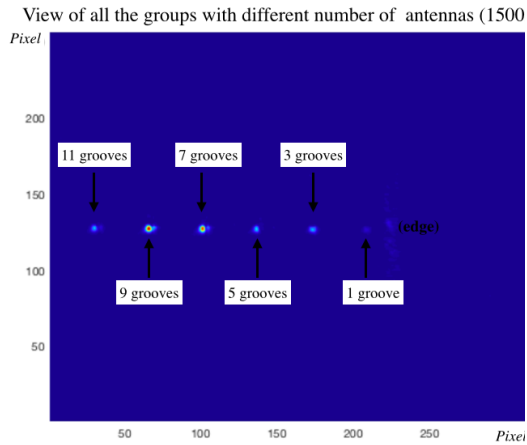


Figure 6. All grooves groups (seen from above)

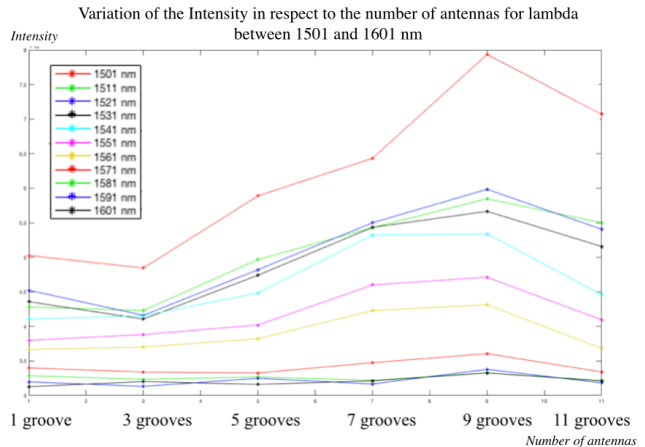


Figure 7. Variation of the signal

The first results show that the group with 11 is not the best, even though the intensity seems to increase with the number of grooves (as expected) Fig 6. Furthermore, a study of the variation of the response as a function of lambda ($\lambda \in [1501; 1601]$) shows that the maximum intensity is around 1500nm rather than 1600nm. That is due to a slight shift in the grooves's pitch that is of 3 μ : as the refractive index is precisely 1,44, the optimal wavelength is 1,44 microns.

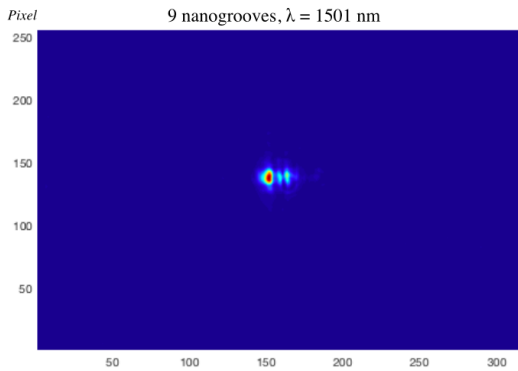


Figure 8. 9 grooves, 3 microns between the grooves and the waveguide

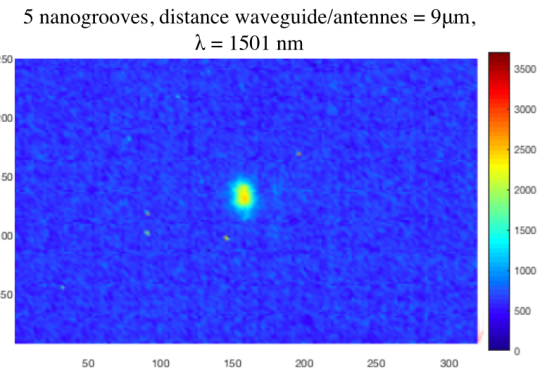


Figure 9. 5 grooves, 9 microns between the grooves and the waveguide

The technology used presents slight repetition errors, leading to the fact that the higher the number of grooves, the more the signal presents several peaks. For the 11 scattering centre antenna, the grooves are not exactly synced anymore, thus creating a contrast loss. This phenomenon can also be seen for 9 grooves, as well as 7 : see Fig 8. Furthermore, as expected, the further away from the grooves the waveguide is, the less intense

the signal is : Fig 9. However, there is no difference between a distance of 0 and a distance of 3 microns because the guided mode is quite large.

The conclusion of this study is that the best combination that we can have is a group of 5 grooves with a 3 microns distance between the antenna and the waveguide :

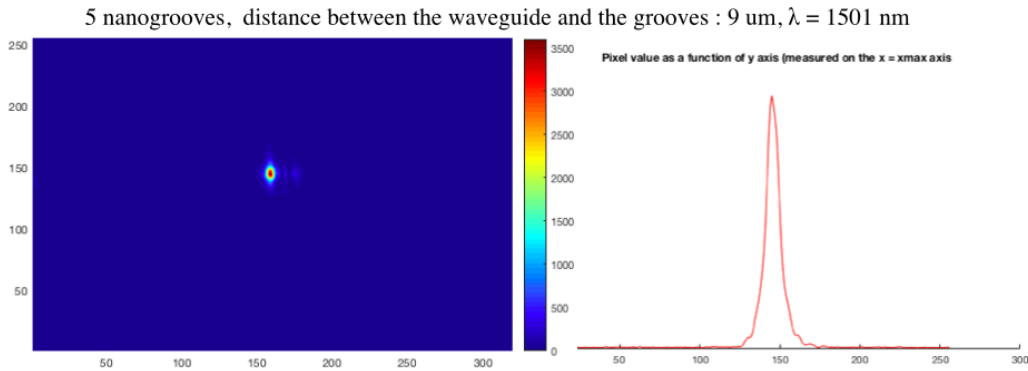


Figure 10. Best combination : 5 grooves, 3 microns depth, 1501 nm

2.2 Vertical radiation pattern of the antennas : propagation (without the mirror)

The first step is to calculate the Bragg order created by the grooves, acting as a grating, in order to have the maximum diffraction angles that we will obtain. The grating law gives us the number of expected Bragg orders in this case :

$$n(sup) * \sin(\theta) = n(ef f) - m \frac{\lambda}{\Lambda}$$

$$\text{with ; } n(sup)=1.444 \quad || \quad -1 \leq \sin(\theta) \leq 1 \quad || \quad n(ef f) = 1.446 \quad || \quad \lambda = 1.55\mu m \quad || \quad \Lambda = 3\mu m \quad (3)$$

From this we can deduce the following inequality :

$$m = \frac{\Lambda}{\lambda} * (n(ef f) - n(sup) * \sin(\theta)) \longrightarrow 0.0039 \leq m \leq 5.5935 \quad (4)$$

As m can only be a integer, there are 5 diffraction orders.

The experimental set-up for the study of the vertical radiation pattern is the following : an IR camera (Hamamatsu) is placed on the sample, where the sampling centres are. This camera was chosen because its pixel matrix can be bared, allowing us to put the matrix directly on the sample, reducing the light's trajectory. It is also a camera that does not require a cooling system which is an advantage when it comes to a compact and simple instrument (as a cooling system might, in some cases, lead to condensation).

The experiment consists in measuring the radiation pattern for different heights of the camera : first the camera is on the sample, then it is raised little by little from $h = 0$ to $h = 520 \mu m$.

The results for the first side (with different number of grooves) are the following :

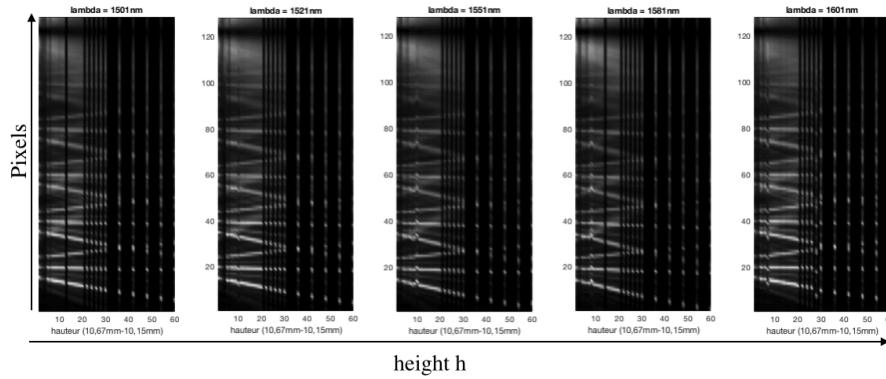


Figure 11. Results for different number of grooves per sampling centre and different wavelengths

The measures were made for the following wavelengths = 1501, 1521, 1551, 1581, 1601 nm. These results show clearly the difference induced by the number of grooves : one groove gives a very wide signal that is indistinguishable from the signal coming from the sampling centre next to it. However, the radiation pattern coming from groups with a higher number of grooves are definite and begin to mix with each other only around a distance of 150 μm between the camera and the sample.

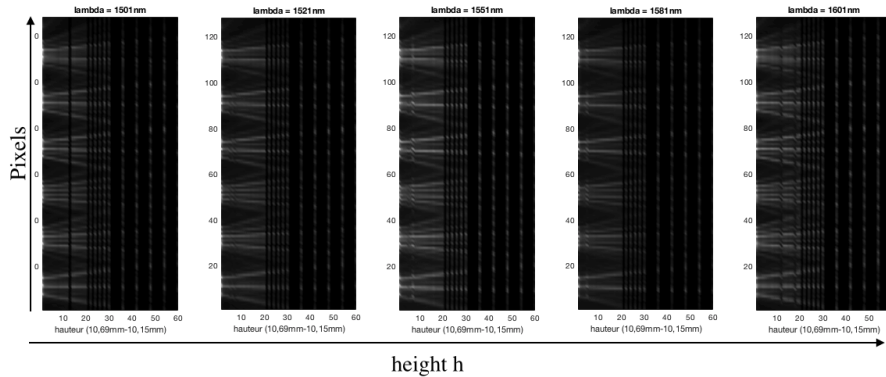


Figure 12. Results for 5 grooves per sampling centre and different wavelengths

Here, each group is clearly distinguishable from its neighbour, and the rays with the maximum diffraction angle meet also only around 150 μm . It is therefore possible to identify the received signals, and to trace them back to the source.

In both case, the predicted Bragg orders are visible. However, all of them are not visible (only 3 or 4 instead of the 5 expected) : that is due to the fact that even though the pixel matrix is bared, there can be a slight air layer remaining between the pixels, causing a total refraction for the higher Bragg orders (with the highest diffraction angle, such as the 5th order : -51.96°)

2.3 Radiation pattern : scanning the SWIFTS effect (with the mirror)

The experimental set-up for those experiments is the same than previously : the Hamamatsu camera is placed on the sample, with the pixel matrix bared. The side of the sample that is studied is the side with 5 grooves per sampling centre, and the mirror has been placed, so there is a stationary wave.

The distance between the camera and the sample is always 0, and the main effect studied is the variation of the wavelength. Different ranges have been studied : from 1520 to 1525nm, from 1530 to 1535 nm, from 1540 to 1545 nm, from 1550 to 1555 nm, and from 1560 to 1565 nm all with a 0,05nm wavelength pitch, and from

1520,3 nm to 1522,3 nm with a 0,01nm pitch. The goal of these experiments is to study the response of each sampling centre to a variation of the wavelength. As each sampling centre is at a given distance from the mirror, the responses should be different :

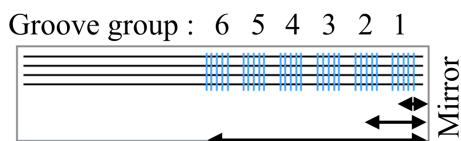


Figure 13.

L : distance of the group to the mirror

$$I \propto \cos \left(2\pi \cdot 2nL / \lambda \right)$$

Figure 14.

As the formula giving the intensity is proportional to the distance of the groove to the mirror (L), the higher the distance, the smaller the period of the wave (increase of the frequency). The results for some of the measurements are the following (with the contrast for each group) : Fig 15, Fig 16, Fig 17, Fig 18 :

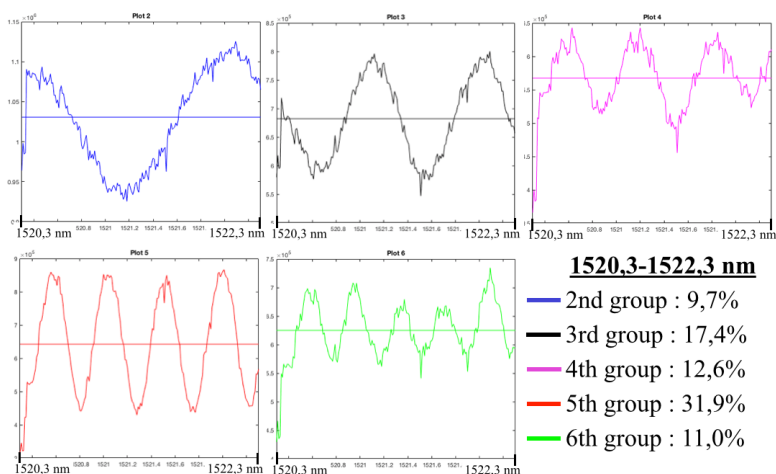


Figure 15. 1520,3 to 1522,3 nm

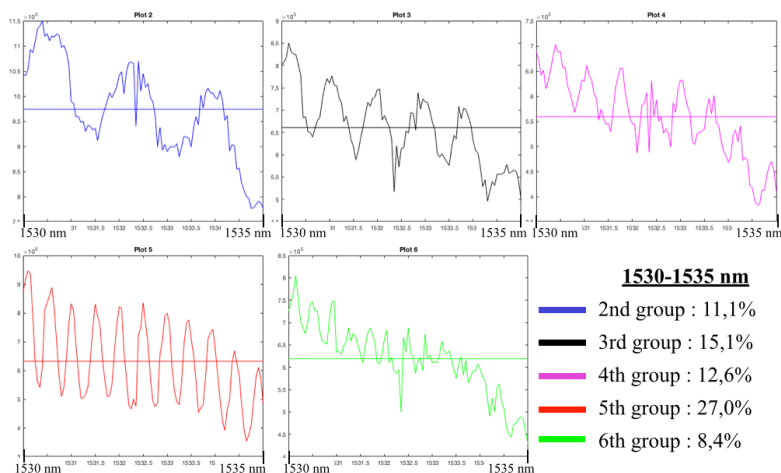


Figure 16. 1530 to 1535 nm

It is clearly visible that the response are different for each scattering group, with the period diminishing with

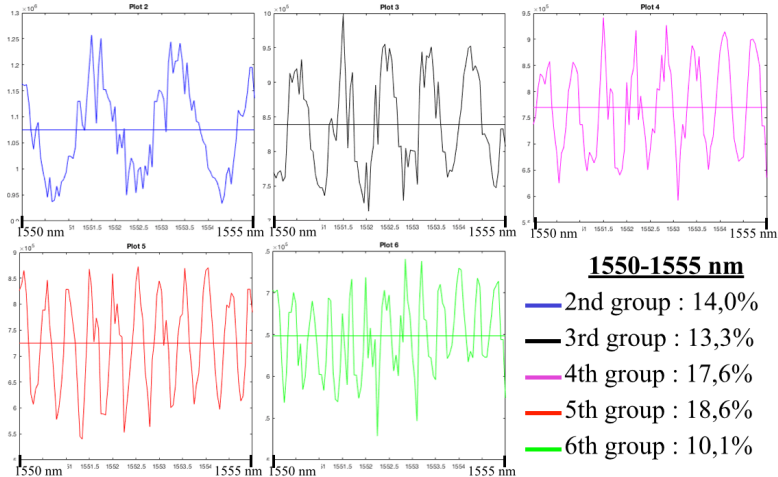


Figure 17. 1550 to 1555 nm

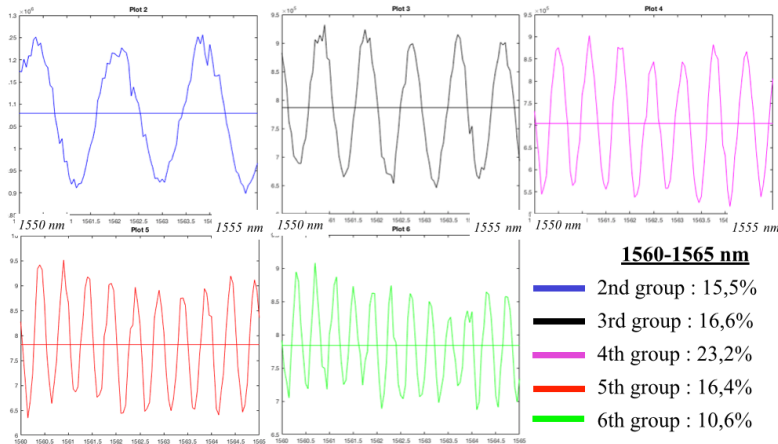


Figure 18. 1560 to 1565 nm

the augmenting distance to the mirror (at the exception of the first group, that was removed because there was too much noise coming from the reflection on the mirror).

The contrast is correct, though much better for the set between 1520 and 1525 than for higher wavelengths. There is also an envelope that will be simulated in the simulation section. In this section, reasons as to why the contrast is not optimal will further be explored.

2.4 Exploitation of the results

In order to study the results given by the sample, another set of experiments was conducted. A data base was created, consisting of 101 measurements (between 1520 and 1525 nm and between 1550 and 1555 nm). In this data base, an "unknown" wavelength was injected, and its value will be retrieved through a comparison algorithm.

For each set of measurements, several "unknown" wavelengths are chosen.

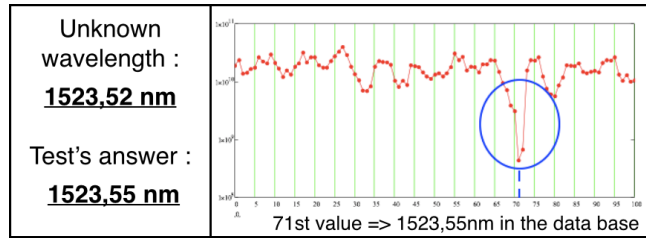


Figure 19. Unknown wavelength : 1523.55nm

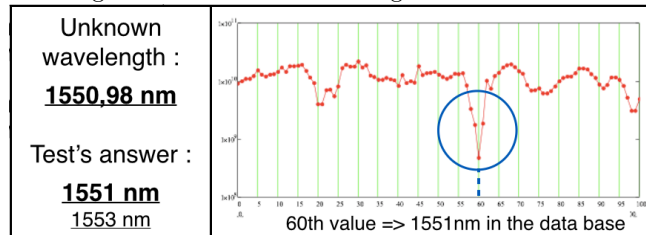


Figure 20. Unknown wavelength : 1550.98nm

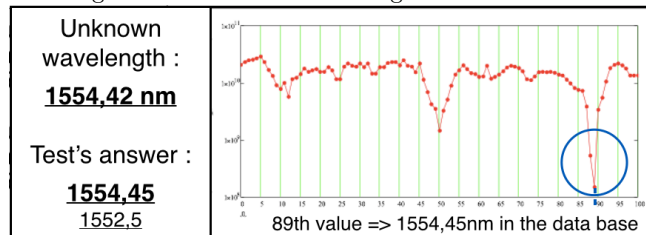


Figure 21. Unknown wavelength : 1554.42nm

These results show that the unknown wavelength can be determined with a high accuracy, around 25 pm : Fig 19, Fig 20. However, there can be two local minimum that do not give the same result : Fig 21, because of aliasing. However, the global minima is still the accurate one, and the unknown value can still be retrieved. In order to test the robustness of the sample, several "unknown" measures were made with a slight change in the injection, and every time the result was still accurate.

	Unknown wavelengths										
Real Value	1520,11	1520,169	1520,37	1520,74	1521,06	1521,96	1522,22	1522,51	1523,01	1523,52	1524,87
Estimation 1 (global min)	1520,75	1521,2	1520,35	1520,7	1521,1	1522	1522,25	1522,5	1523,0	1523,55	1524,85
Estimation 2 (local min)	/	/	1522,25	1522,65	1522,95	1523,9	/	/	/	/	/

Figure 22. Comparison unknown wavelength/estimated result – 1520-1525 nm

	Unknown wavelengths											
Real Value	1550,23	1550,26	1550,66	1550,87	1550,98	1551,169	1551,32	1552,97	1553,279	1553,63	1554,42	1554,86
Estimation 1 (global min)	1550,2	1550,3	1550,65	1550,85	1551	1551,2	1551,25	1553,0	1553,3	1553,65	1554,45	1554,85
Estimation 2 (local min)					1553	1553,05	1551,35				1552,5	1552,9

Figure 23. Comparison unknown wavelength/estimated result – 1550-1555 nm

All the unknown wavelength were retrieved with this method, and even though sometimes there were several minima, the global minima still gave the right value.

3. SIMULATIONS

As previously seen, the contrast is correct but not perfect. There are several reasons as to why the contrast is not optimal : the presence of Bragg orders, and the fact that these Bragg orders are asymmetric. As previously calculated there are 5 Bragg orders, though only 4 are clearly visible because of the total refraction between air and glass. As these orders are thin, the slightest asymmetry will result in a bad superposition between the incoming and reflected wave, and ultimately in a diminished contrast.

In order to illustrate that, simulations were made using a program that allows the simulations of 1 sampling centre, with a number of parameters that can be changed (size of the grooves, number of grooves, wavelength, materials, distance to the mirror (L), the burial depth of the waveguide and the grooves). The simulation gives the result either still in the sample (just before the glass/air interface), or on the pixels of the detector above, meaning that the light has crossed the air layer and the semi-conductor of the detector.

The following simulation is that of a 5 grooves sampling centre, for 1550nm, and show the result on the pixel detector. The sampling centre is the 5th one (see 13), and the air layer is of 5 μm .

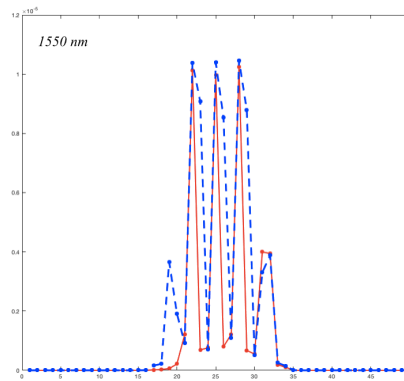


Figure 24. Superposition of : the incoming wave only (red) and the returning wave (blue) on the pixel matrix

This figure shows the 4 expected Bragg orders, with one being significantly smaller than the others (explaining why there were only 3 main Bragg orders seen on 11 and 12). It is also obvious that the superposition is far from being perfect : the signal is not symmetric, and there is a slight offset between the incoming and returning wave. Assuming that the offset is due to the fact that the pitch between two grooves of the same sampling centre is $3\mu\text{m}$ and not exactly $3 * \frac{\lambda}{n} = 3 * \frac{1,55}{1,44} = 1,22$, another simulation was made to compare different wavelengths. The results are still in the sample, for a 5 grooves sampling centre, with the incoming and returning wave :

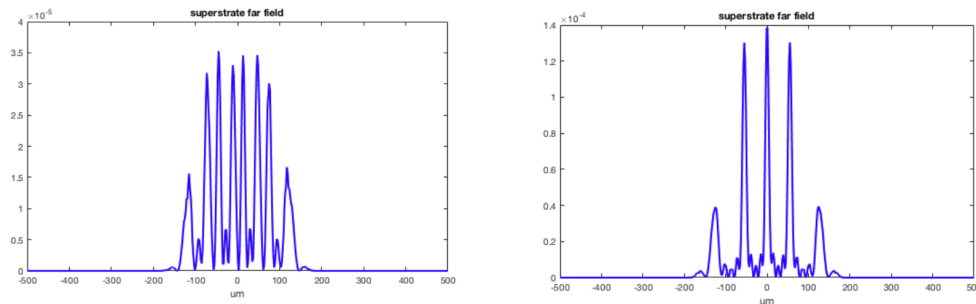


Figure 25. With the mirror (total reflection) : Simulation at 1550nm still in the sample
 Figure 26. With the mirror (total reflection) : Simulation at 1446 nm still in the sample

At 1550nm, there are several Bragg orders, more than the 5 expected because of the bad superposition between the incoming Bragg orders and the returning ones. However, at 1446nm, the Bragg orders are perfectly overlapped with each other.

In order to get rid of the Bragg orders, the pitch between the grooves should be diminished up to $1,07 \text{ nm} \left(\frac{\lambda}{n}\right)$. Simulations were made to determine what the result would be with a $1 \text{ }\mu\text{m}$ pitch, here a 5 grooves group with the signal on the detector.

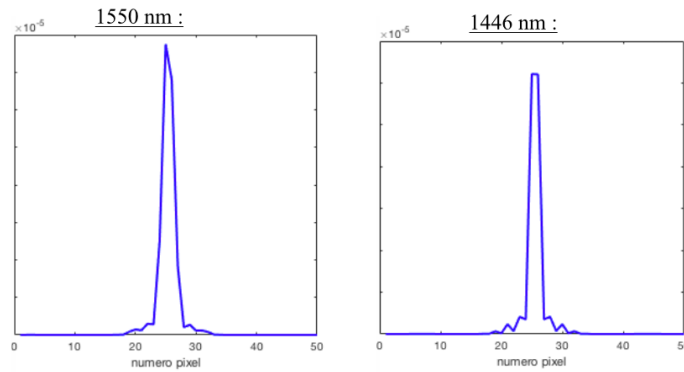


Figure 27. 5 grooves with a 1 micron pitch, for 1550 and 1446nm

It is clear that there is only one Bragg order, and that the overlapping would be better because of the symmetry of the signal. However, the technology does not allow for a pitch under 3 microns. Therefore, in order to see if the contrast could be improved, several simulations were made to determine the contrast envelope in the 1450-1600 nm range.

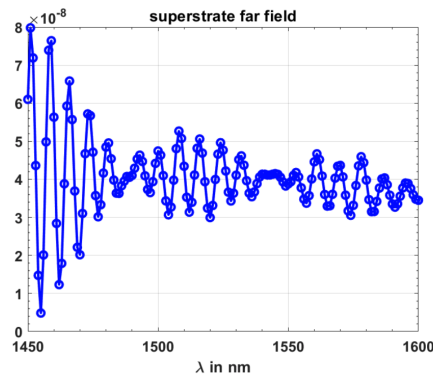


Figure 28. Contrast for a 3 microns pitch, signal with a total reflection (mirror)

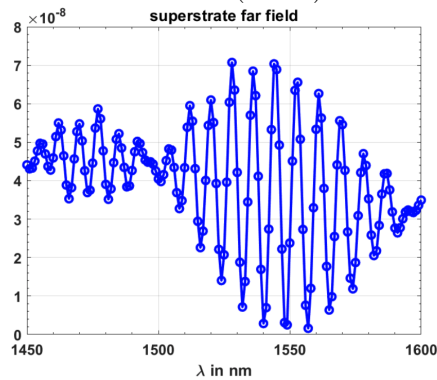


Figure 29. Contrast for a 3,22 microns pitch, signal with a total reflection (mirror)

On 28, the envelope is better around 1450nm than 1550, because $3 \mu m$ is not the perfect pitch between two grooves. this figure corresponds exactly to the observation made during the experiments : the contrast seemed to be higher for a lower wavelength (around 1450nm). Furthermore there was a distinct contrast envelope different for each wavelength : for instance the shape of the signal was clearly going downwards for the span between 1530 and 1535nm (16).

On this figure (28), the best contrast in the 1500-1550 range is around 1520nm (second oscillation). Roughly calculated, the contrast here at 1520nm is around 30, as it was in the experiments.

On 29, the contrast is the best around 1550nm, as expected. The pitch is exactly $3 * \frac{\lambda}{n}$, and the best contrast is around 90 , which leads to believe that for a pitch of 3,22 microns, the contrast obtained by the antennas, despite the Bragg orders could be up to 90, though on a small bandwidth. It is a compromise between the number of grooves and the bandwidth.

As the technology does not allow the pitch between the grooves to be under 3 microns, going above 3 microns would be a solution for a better contrast.

4. CONCLUSION AND PERSPECTIVES

The technology that we used (ultrafast laser writing) has its limitations (pitch between the grooves), but presents many advantages : it is a simple, low cost technology, that allows 3D printing and buried waveguide. The sample are therefore compact and easily handled. Furthermore, the choice of the material (borosilicate) also gives a simple and low cost sample.

Even though there are Bragg orders in the extracted result, the signal can be exploited and an unknown wavelength can be retrieved. The sample can be used as a lambdameter with a very high resolution (around 25pm), though on small windows (around 2nm). The contrast is correct, and can easily be improved, as shown by simulations. Considering that the sample only has 6 sampling centres, the Bragg orders, and that the contrast can be improved, the sample show promising outcomes for future improvements.

One of the main directions that the project will take is the change of the material. An electro-optical material is considered (Lithium Niobate). An electro-active material will allow a temporal offset in addition to a temporal offset, which will improve the scanning effect.

Changing the technology used for the grooves and the waveguide is another parameter that can be explored.

ACKNOWLEDGMENTS

Authors acknowledge the funding from ASHRA (Action Spécifique Haute Resolution Angulaire) from INSU-CNRS and LabEx FOCUS ANR-11-LABX-0013

REFERENCES

- [1] : G. Martin, J. R. Vázquez de Aldana, A. Rodenas, C. d'Amico, R. Stoian, "Recent results on photonic devices made by laser writing: 3D 3T near IR waveguides, mid-IR spectrometers and electro-optic beam combiners," Proc. SPIE 9907, Optical and Infrared Interferometry and Imaging V, 990739 (26 July 2016)
- [2] : E. le Coarer, S. Blaize, P. Benech, I. Stéfanon, A. Morand, G. Lérondel, G. Leblond, P. Kern, J. Fédéli, P. Royer, "Wavelength-scale stationary-wave integrated Fourier-transform spectrometry". Nature Photon 1, 473–478 (2007)
- [3] : A. Morand, I. Heras, G. Ulliac, E. Le Coarer, P. Benech, N. Courjal, and G. Martin, "Improving the vertical radiation pattern issued from multiple nano-groove scattering centers acting as an antenna for future integrated optics Fourier transform spectrometers in the near IR," Opt. Lett. 44, 542-545 (2019)
- [4] : R. Stoian, M. Bhuyan, G. Cheng, G. Zhang, R. Meyer, and F. Courvoisier "Ultrafast Bessel beams; advanced tools for laser material processing" Adv. Opt. Technolog. 7, 165 (2018)